JOURNAL OF MAGNETIC RESONANCE 76, 106–120 (1988)

Oxygen-17 Cross-Polarization NMR Spectroscopy of Inorganic Solids*

THOMAS H. WALTER, GARY L. TURNER, AND ERIC OLDFIELD†

School of Chemical Sciences, University of Illinois at Urbana-Champaign, 505 South Mathews Avenue, Urbana, Illinois 61801

Received May 14, 1987

We have obtained ^{17}O nuclear magnetic resonance spectra of a variety of ^{17}O-labeled solids ($Mg(OH)_2$, $Ca(OH)_2$, boehmite (AlO(OH)), talc ($Mg_3Si_4O_{10}(OH)_2$), $(C_6H_5)_3SiOH$, and amorphous SiO_2) using high-field static and "magic-angle" sample spinning techniques, together with ^1H cross polarization and dipolar decoupling. Our results show that large cross-polarization enhancements can be obtained and that reliable second-order quadrupolar powder lineshapes can be observed under cross-polarization conditions. We have also investigated the dynamics of cross polarization for several samples, including measurements of cross-relaxation rates and ^1H and ^{17}O rotating-frame spin–lattice relaxation times. We show that rapid ^{17}O rotating-frame spin–lattice relaxation reduces the cross-polarization enhancement in some cases and that differences in cross-relaxation rates can be used to "edit" spectra by selectively enhancing protonated oxygen resonances (in general, hydroxide versus oxide ions, in inorganic solids). When applied to high surface area metal oxides such as amorphous silica, this selectivity enables the observation of resonances from surface hydroxyl groups that are difficult to detect by conventional ^{17}O NMR. Overall, the cross-polarization approach appears to have considerable utility for aiding in the interpretation of ^{17}O NMR spectra of complex inorganic solids.

INTRODUCTION

The nuclear magnetic resonance active nuclide oxygen-17 ($I = \frac{5}{2}$, 0.037% natural abundance, $\gamma = -0.5793$ kHz/G) should, in principle, be a valuable probe for studying the structure and reactivity of a variety of inorganic solids, such as heterogeneous catalysts, glasses, ceramics, and various mineral phases. It has recently been shown that useful information can indeed be obtained from solid-state ^{17}O NMR studies of a variety of isotopically enriched minerals and zeolites by observing the central ($\frac{1}{2}$, $-\frac{1}{2}$) transition in high magnetic fields (*1–9*). In most cases, the dominant effect in solid-state ^{17}O NMR spectra is the quadrupole interaction, which broadens the central transition only to second order, resulting in linewidths on the order of 5–25 kHz for polycrystalline samples, at 11.7 T. These linewidths may be partially reduced by rapid "*m*agic-*a*ngle" *s*ample *s*pinning (MASS), often allowing facile resolution of nonequivalent sites in complex samples (*2, 9*). It has been shown elsewhere that, as expected,

* This work was supported by the U.S. National Science Foundation Solid-State Chemistry Program (Grant DMR 86-40075, T.H.W.), the National Institutes of Health (HL-19481), and in part by the Mobil Foundation.

† To whom correspondence should be addressed.

0022-2364/88 $3.00

the nuclear quadrupole coupling constant (e^2qQ/h) and the asymmetry parameter (η) of the electric field gradient tensor, as well as the isotropic chemical shift (δ_i), are sensitive to the local electronic environment of the oxygen site (*2, 6, 10*).

To extend the utility of solid-state ^{17}O NMR we have recently been exploring the potential of ^{17}O–^{1}H cross polarization, in conjunction with dipolar decoupling and MASS. Cross polarization of the relatively insensitive ^{17}O nucleus offers the possibility of large sensitivity enhancements, allowing the use of either lower isotopic enrichment levels or shorter acquisition times. In this publication we report the results of a series of cross-polarization experiments on several ^{17}O-labeled inorganic solids. Our results demonstrate large sensitivity enhancements and show that cross polarization may be used to "edit" ^{17}O spectra on the basis of the presence of directly bonded protons. This sensitivity enhancement and selectivity not only permits facile assignment of "protonated" versus "nonprotonated" oxygens in inorganic solids, but also allows ready observation of hydroxyl groups present on the surfaces of high surface area oxides, such as amorphous silica.

EXPERIMENTAL METHODS

Nuclear magnetic resonance spectroscopy. Oxygen-17 NMR spectra were obtained on FT NMR spectrometers operating at 67.8 and 48.8 MHz, using Oxford Instruments (Osney Mead, Oxford, United Kingdom) 11.7 T, 52 mm bore or 8.45 T, 89 mm bore superconducting solenoid magnets. Nicolet Instrument Corp. (Madison, Wisconsin) Model 1280 computer systems were used for data acquisition, Amplifier Research (Souderton, Pennsylvania) Model 200L and 150LA amplifiers for radiofrequency (RF) pulse generation, and Henry Radio (Los Angeles, California) Model 70D02 and 1002A amplifiers for final ^{1}H RF pulse generation. Static and MASS NMR spectra at both field strengths were obtained using Doty probes (Doty Scientific, Columbia, South Carolina). ^{1}H and ^{17}O RF field strengths were typically 50 and 16.7 kHz, respectively, and were adjusted for optimal cross polarization by observing the resonance from ^{17}O-enriched $Ca(OH)_2$. Cross-polarization spectra were obtained using the single contact spin-lock method (*11*), with spin temperature alternation (*12*) to eliminate signals not arising via cross polarization. Chemical shifts are reported in parts per million from an external sample of water, with low-field, high-frequency, paramagnetic, deshielded values being designated as positive, in accord with the IUPAC (δ scale) convention. Quadrupole coupling constants, asymmetry parameters, and chemical shifts were obtained by computer simulation of the experimental spectra. Cross-relaxation rates and ^{1}H rotating-frame spin–lattice relaxation times ($T_{1\rho}$) were determined by least-squares fitting of integrated signal intensity versus contact time data to Eq. [2]. Oxygen-17 $T_{1\rho}$ values were measured using the pulse sequence described by Stejskal *et al.* (*13*) for determining ^{13}C $T_{1\rho}$ values, and ^{17}O spin–lattice relaxation times were measured using the saturating comb saturation-recovery method (*14, 15*).

Chemical aspects. Samples were enriched to 10–50% in ^{17}O either by direct synthesis or by exchange with $H_2{}^{17}O$ at 95–105°C in commercial pressure vessels (Parr Instrument Co., Moline, Illinois). ^{17}O-enriched $Mg(OH)_2$ was prepared by treating $Mg(NO_3)_2$ with KOH dissolved in 20 at.% $H_2{}^{17}O$ (Cambridge Isotopes, Woburn, Massachusetts), followed by washing with water and drying at 120°C for 12 h. ^{17}O-enriched $Ca(OH)_2$

was prepared in a similar manner from $CaCl_2$ and $KOH/H_2{}^{17}O$. ^{17}O-enriched boehmite (AlO(OH)) was prepared by treating commercial boehmite (CATAPAL, Conoco Chemicals, Houston, Texas) with $H_2{}^{17}O$ (20%) for 24 h at 105°C, followed by drying at 120°C. ^{17}O-enriched amorphous silica was prepared by the hydrolysis of $SiCl_4$ with $H_2{}^{17}O$ (50%), as described by Geissberger and Bray (*16*), followed by drying at 120°C. Enriched talc ($Mg_3Si_4O_{10}(OH)_2$) was the generous loan of Mr. C. Weiss, Jr., and Professor R. J. Kirkpatrick, and ^{17}O–$(C_6H_5)_3SiOH$ was lent by Dr. S. Schramm and Dr. Kirk Schmitt. The purity of each sample was verified by powder X ray diffraction and by chemical analysis.

RESULTS AND DISCUSSION

General aspects. While cross-polarization experiments involving polarization transfer from ^1H to spin-$\frac{1}{2}$ nuclei such as ^{13}C (*11*), ^{15}N (*17*), ^{29}Si (*18*), ^{31}P (*19*), and ^{113}Cd (*20*) have now become routine, there have so far been relatively few reports of cross polarization from ^1H to quadrupolar nuclei. The cross-polarization behavior of such systems is complicated by the presence of a generally strong nuclear quadrupole interaction. For example, for integer spin nuclei such as ^{14}N ($I = 1$), the cross-polarization match condition has been shown to be strongly dependent on the quadrupole frequency, leading to different match conditions for different orientations in a polycrystalline sample, and thus to a distorted powder pattern (*21*). For this reason cross-polarization experiments involving quadrupolar nuclei have been almost exclusively restricted to single crystal samples (*22–24*). For noninteger spin nuclei, however, it is possible to observe essentially undistorted second-order quadrupolar lineshapes for the central $(\frac{1}{2}, -\frac{1}{2})$ transition in powder samples (*25–27*). The match condition can be predicted from the Hartmann–Hahn equation (*28*):

$$\alpha_a\gamma_a H_{1a} = \alpha_b\gamma_b H_{1b}, \qquad [1]$$

where γ_i and H_{1i} are the gyromagnetic ratio and RF field strength for nucleus i, and $\alpha = [I(I+1) - m(m-1)]^{1/2}$ for a transition between the levels m and $(m-1)$. When both nuclei have $I = \frac{1}{2}$, this equation reduces to the familiar form $\gamma_a H_{1a} = \gamma_b H_{1b}$. However, for cross polarization of the $(\frac{1}{2}, -\frac{1}{2})$ transition of ^{23}Na ($I = \frac{3}{2}$), Vega (*24*) has demonstrated that the match condition $2\gamma_{Na}H_{1Na} = \gamma_H H_{1H}$, holds, while for observation of the $(\frac{1}{2}, -\frac{1}{2})$ transition for ^{17}O ($I = \frac{5}{2}$), we find the match condition to be $3\gamma_O H_{1O} = \gamma_H H_{1H}$, in agreement with Eq. [1]. These conditions amount to matching the ^1H 90° pulse length to the "solid" ^{23}Na or ^{17}O 90° pulse lengths, which are smaller than the solution values by the same factor α when only the central transition is observed (*29*). For example, with a ^1H 90° pulse length of 5 μs ($\gamma_H H_{1H} = 50$ kHz) we observe optimum cross polarization when $\gamma_O H_{1O} = 16.7$ kHz, which corresponds to a "solution" ^{17}O 90° pulse length of 15 μs, but to a "solid" ^{17}O 90° pulse length of 5 μs.

To illustrate the large signal-to-noise enhancements that can be obtained by cross polarization, we show in Fig. 1 ^{17}O NMR spectra of a stationary sample of $Mg(OH)_2$, which exhibits a second-order quadrupolar powder pattern from a single oxygen site. Figure 1A shows the results of a cross-polarization experiment, while for comparison we show in Fig. 1B the conventional proton-decoupled ^{17}O NMR spectrum of the same sample. Figure 1C shows a computer simulation of this powder pattern, using

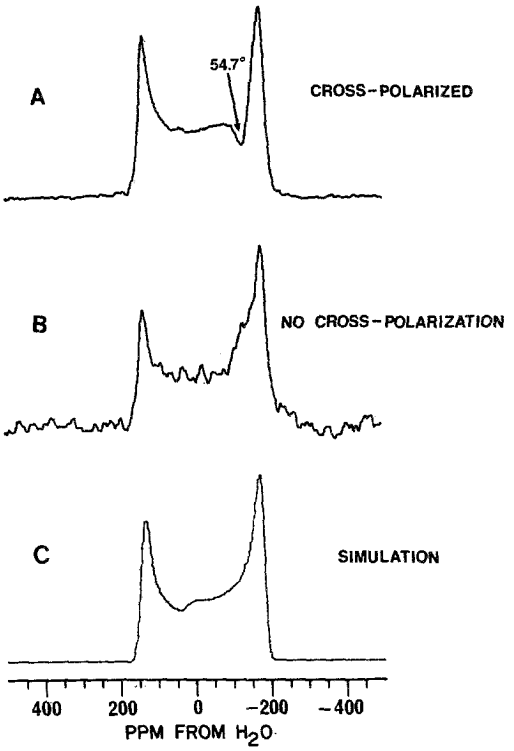

FIG. 1. Static ^{17}O NMR spectra of polycrystalline $Mg(OH)_2$ obtained at 67.8 MHz. (A) Cross-polarized spectrum with proton decoupling: 200 scans, 1 ms contact time, 5 s recycle time. (B) Proton-decoupled spectrum without cross polarization: 200 scans, 5 s recycle time. (C) Simulated second-order quadrupolar powder pattern using e^2qQ/h = 6.8 MHz, η = 0.0, δ_i = 25 ppm.

a quadrupole coupling constant of 6.8 MHz, an asymmetry parameter of 0.0, and an isotropic chemical shift of 25 ppm. The results shown in Fig. 1 indicate a cross-polarization enhancement of 6.2, demonstrating that it is possible to obtain enhancements close to the theoretical maximum, given by the ratio of gyromagnetic ratios: γ_H/γ_O = 7.38. It can also be seen that the only distortion in the quadrupolar powder pattern caused by cross polarization is a "notch" in the lineshape slightly downfield from the high-field singularity. From the angular dependence of the second-order quadrupolar shift (*30*) we find that the "notch" corresponds to those sites that have the z component of the electric field gradient tensor (V_{zz}) oriented at 54.7° (the "magic angle") to the static magnetic field. Since each oxygen in $Mg(OH)_2$ is coordinated to three magnesium cations and one hydrogen in a site with threefold symmetry (*31*), V_{zz} is constrained to lie along the O–H bond. Thus sites oriented with V_{zz} tipped at 54.7° to the magnetic field also have the O–H bond tipped at 54.7°, an orientation for which the nearest neighbor ^{17}O–^1H dipolar interaction vanishes. Consequently, for these oxygen sites the cross-relaxation rate (which is proportional to the strength of the dipolar coupling) is governed not by the directly bound proton, but by the next nearest protons (located several angstroms away), so that a much longer time is required for complete cross polarization. Consistent with this hypothesis, we find that the "notch" is not as prom-

inent at longer contact times (although it is still evident after 25 ms) and that $Ca(OH)_2$, which is isostructural with $Mg(OH)_2$ (*32*), exhibits an identical distortion. This effect is a manifestation of the orientation dependence of cross-relaxation rates and has also been observed in chemical-shift anisotropy powder patterns in ^{13}C cross-polarization experiments on static samples (*11*).

Cross-polarization dynamics. An understanding of the cross-polarization behavior of complex systems requires some knowledge of the cross-relaxation rates and relaxation times which govern the buildup and decay of the cross-polarized signal intensity. We have thus investigated the dynamics of ^{17}O cross polarization for several compounds. As illustrated in Fig. 2 for the two oxygen sites of boehmite (vide infra), we find that the dependence of the integrated signal intensity (I) on the contact time (t) can be fitted reasonably well by an equation of the conventional form (*33*), characterized by a cross-relaxation time constant T_{OH} (which governs the signal buildup) and a ^1H rotating-frame spin–lattice relaxation time $T_{1\rho}^H$ (which governs the signal decay):

$$I(t) = I_{max}(1 - T_{OH}/T_{1\rho}^H)^{-1}[\exp(-t/T_{1\rho}^H) - \exp(-t/T_{OH})]. \quad [2]$$

We note, however, that the assumptions involved in the derivation of this equation may not all be valid for the cases considered here, and consequently the experimentally determined cross-relaxation rates and rotating-frame relaxation times should be considered as effective values (indicated by $'$). This point is discussed in detail in the Appendix.

As shown in Table 1, we find T'_{OH} values on the order of 20–40 μs for hydroxyl oxygens in two different inorganic solids. These short cross-relaxation time constants reflect the strong ^{17}O–^1H dipolar coupling that arises from the short (~1 Å) O–H bonds and are comparable to those of rigid C–H moieties in ^{13}C-CPMAS (*34*). No T_{OH} values are given in Table 1 for $Ca(OH)_2$ and $Mg(OH)_2$ because they show pro-

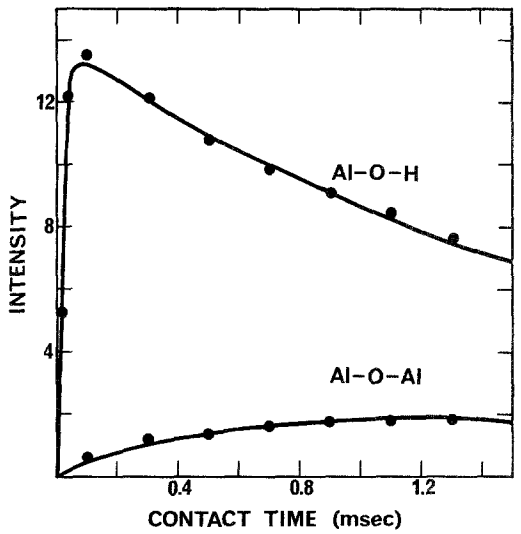

FIG. 2. Plot of peak intensity (in arbitrary units) versus cross-polarization contact time for the two oxygen sites of boehmite; the solid lines represent least-squares fits to Eq. [2].

TABLE I

Cross-Relaxation Rates, Rotating-Frame Spin–Lattice Relaxation Times, and Spin–Lattice Relaxation Times for Several Inorganic Solids[a]

Sample	Site	T'_{OH} (ms)	$T^{H'}_{1\rho}$ (ms)	$T^{O}_{1\rho}$ (ms)	T_1 (^{17}O) (s)
$Ca(OH)_2$	Ca–O–H	—[b]	250 (±10)[c]	870 (±5)	6.2 (±0.2)
$Mg(OH)_2$	Mg–O–H	—[b]	69 (±2)	230 (±5)	0.98 (±0.05)
AlO(OH)[d]	Al–O–H	0.018 (±0.002)	2.1 (±0.1)	0.125 (±0.005)	0.15 (±0.05)
	Al–O–Al	0.60 (±0.05)	2.3 (±0.1)	—	2.6 (±0.1)
Amorphous SiO_2	Si–O–H	0.042 (±0.005)	25 (±1)	0.27 (±0.01)	2.9×10^{-4} ($\pm 0.6 \times 10^{-4}$)
	Si–O–Si	1.4 (±0.1)	25 (±1)	28 (±2)	0.022 (±0.002)

[a] Measured at room temperature at 11.7 T without magic-angle spinning, unless otherwise noted.
[b] Unmeasurable due to oscillation.
[c] Estimated error limits based on standard deviations from least-square fits and reproducibility of replicate measurements.
[d] Measured on a sample spinning at the magic angle at 6.0 kHz.

nounced oscillations in their contact time dependence, as illustrated in Fig. 3. These oscillations, which have previously been observed in ^{13}C cross-polarization experiments (*35*), occur whenever there is a single dominant dipolar interaction in a spin system,

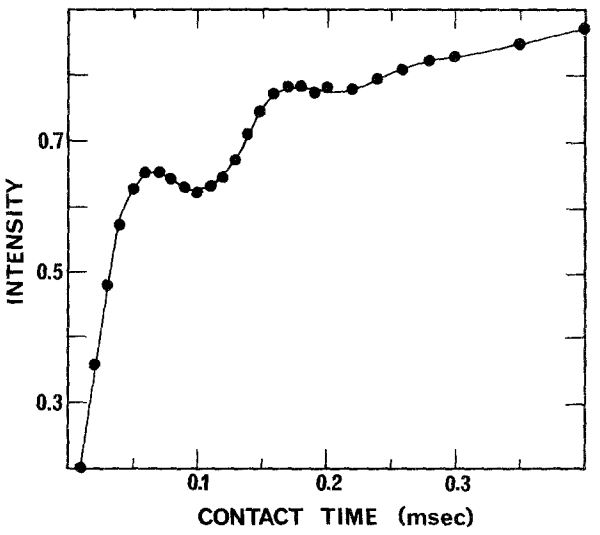

FIG. 3. Plot of integrated signal intensity (relative to the maximum value) versus cross-polarization contact time for a stationary sample of polycrystalline $Ca(OH)_2$.

and we therefore attribute them to the large nearest-neighbor ^{17}O–^{1}H dipolar coupling in these hydroxides. (This is also responsible for the orientation-dependent cross-relaxation rate which causes the lineshape distortion discussed above.) Müller *et al.* (*35*) have shown that the frequency of the transient oscillations is related to the dipolar coupling constant. The data shown in Fig. 3 give a powder average coupling constant of 16.7 kHz, from which we can calculate an O–H bond length of 0.92 Å, in good agreement with the value of 0.936 Å determined by neutron diffraction (before correction for vibrational motion) (*32*). Note that although the maximum intensity for $Ca(OH)_2$ and $Mg(OH)_2$ is not obtained until approximately one millisecond, the intensity reaches 65% of the maximum by 65 μs, so that these hydroxides behave as if they have cross-relaxation time constants on the order of 20 μs. In contrast to the short T'_{OH} values found for hydroxyl oxygens, nonhydroxyl oxygens show T'_{OH} values that are much larger as a consequence of the weaker ^{17}O–^{1}H dipolar coupling. As illustrated below, these large differences in cross-relaxation rates for hydroxyl versus nonhydroxyl oxygens can be exploited to observe hydroxyl sites selectively in complex samples.

The proton $T'_{1\rho}$ data in Table 1 cover a wide range of values, from 2.1 ms in boehmite to 250 ms in $Ca(OH)_2$. With the exception of boehmite, these $T^{H'}_{1\rho}$ values are sufficiently long to allow the full cross-polarized signal intensity to be obtained before rotating-frame spin–lattice relaxation becomes significant. We have also measured ^{17}O $T_{1\rho}$ values ($T^{O}_{1\rho}$) for these compounds to see if the efficient quadrupolar relaxation mechanism, which frequently results in short ^{17}O T_1's in the solid state, produces correspondingly short $T^{O}_{1\rho}$ values. Since T_1 and $T_{1\rho}$ are affected by motions on different time scales (*36*), there is not necessarily a simple correlation between $T_1(^{17}O)$ and $T^{O}_{1\rho}$. However, because spin–lattice relaxation occurs concomitantly with rotating-frame spin–lattice relaxation, $T_{1\rho}$ can be no longer than T_1. Thus while we observe long $T^{O}_{1\rho}$ values for $Ca(OH)_2$ and $Mg(OH)_2$, which have relatively long ^{17}O T_1's, we find very short $T^{O}_{1\rho}$ values for the hydroxyl sites of boehmite and silica, which have short ^{17}O T_1's.

As discussed in the Appendix, when $T^{O}_{1\rho}$ is short Eq. [2] is no longer valid, although a similar equation can be derived to take account of $T^{O}_{1\rho}$ effects. The theoretical consequences of rapid $T^{O}_{1\rho}$ relaxation are that the ^{17}O magnetization cross polarizes at a faster rate, but the maximum intensity attained is smaller. The latter result can be rationalized by considering that when $T^{O}_{1\rho}$ is short there is competition between the simultaneous buildup of the ^{17}O magnetization by cross polarization and its decay by rotating-frame spin–lattice relaxation, so that the full intensity is never attained. It is important to note, however, that the fall off in intensity at long contact times is still governed by the proton $T_{1\rho}$, regardless of how short $T^{O}_{1\rho}$ is. Thus efficient $T^{O}_{1\rho}$ relaxation does not make cross polarization impossible, but only reduces the enhancement factor. In agreement with these predictions, we have observed cross-polarization enhancement factors that are substantially less than the theoretical maximum of 7.38 for sites with short $T^{O}_{1\rho}$ values. As noted in the Appendix, however, this may also be attributed in part to the fact that ^{17}O is not a rare spin in these highly enriched samples.

Spectral editing. While the signal-to-noise enhancement provided by cross polarization often results in dramatic reductions in data acquisition time, we believe that the major utility of ^{17}O cross polarization lies in its ability to discriminate between

oxygens bearing hydrogen versus those without directly bonded hydrogen (protonated and nonprotonated oxygens, to borrow terminology from the ^{13}C area), based on differences in their cross-relaxation rates. As an example of the selectivity of the ^{17}O cross-polarization experiment, we show in Fig. 4A the ^{17}O MASS NMR spectrum of an ^{17}O-enriched sample of the aluminum oxide hydroxide boehmite (AlO(OH)), which has two equally abundant oxygen sites: Al–O–Al and Al–O–H (*37*). We assign the resonance at 70 ppm to the Al–O–Al site based on its similarity to the oxygen resonance of α-Al_2O_3 (*2*), in which this is the only type of site, and the broader resonance near 0 ppm is therefore assigned to the Al–O–H site. When a cross-polarization spectrum is recorded for the same sample, only the hydroxyl resonance is observed when a short contact time is used (Fig. 4B). The explanation for this is evident from the contact time dependence shown in Fig. 2. While the hydroxyl oxygen resonance, with its short T'_{OH}, reaches maximum intensity at 0.1 ms, the Al–O–Al resonance builds up much more slowly. Furthermore, due to the unusually short $T_{1\rho}^{H'}$ of this compound, the full intensity of the Al–O–Al resonance is never obtained by cross polarization, since rotating-frame relaxation destroys the resonance before it has time to build up. This experiment demonstrates how large differences in cross-relaxation rates for protonated versus nonprotonated oxygens can be exploited to make specific spectral assignments in inorganic solids.

Oxygen-17 spectral editing may be extended to more complicated systems, such as the mineral talc ($Mg_3Si_4O_{10}(OH)_2$), which has the structure shown below, with three chemically distinct oxygen sites: Si–O–Mg, Si–O–Si, and Mg–O–H, in a 2:3:1 ratio (*38*):

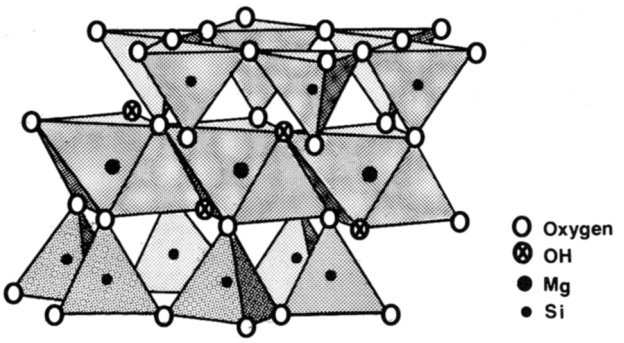

As shown in Fig. 5A, the overlap of second-order quadrupolar powder patterns from these three sites results in a complicated spectrum that can, however, be closely simulated using three axially symmetric second-order quadrupolar powder patterns in a 2:3:1 ratio, as shown in Fig. 5C. The quadrupole coupling constants and isotropic chemical shifts (see legend to Fig. 5) found for the Si–O–Mg and Si–O–Si sites are similar to the values observed for these same nearest-neighbor environments in other silicate minerals (*2, 9*), while the Mg–O–H site is similar to the oxygen site in $Mg(OH)_2$ (vide supra). Figure 5B demonstrates that cross polarization can be used to observe the hydroxyl resonance even in this extensively overlapped spectrum, supporting the simulation and assignments of Fig. 5C. At the very short contact time necessary to obtain this spectrum, the intensity distortions resulting from the orientation dependence

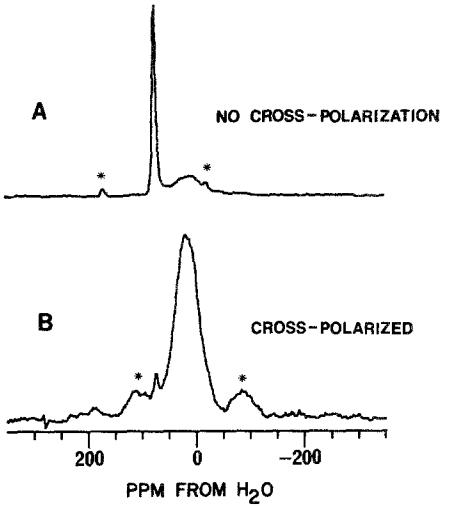

FIG. 4. MASS ^{17}O NMR spectra of boehmite obtained at 67.8 MHz. (A) Proton-decoupled spectrum without cross polarization: 2000 scans, 1 s recycle time, 5.2 kHz spinning speed. (B) Cross-polarized spectrum: 0.1 ms contact time, 2000 scans, 1 s recycle time, 5.2 kHz spinning speed (* indicates spinning sidebands).

of T_{OH} are particularly noticeable. The locations of the powder pattern singularities, however, are not altered by this effect.

Surface hydroxyls. While the selectivity afforded by ^{17}O cross polarization should prove useful in the interpretation of the ^{17}O NMR spectra of complex bulk inorganic solids, it can also be exploited to study the hydroxylated surfaces of high surface area oxides, such as amorphous silicas and transitional aluminas, which are widely used as both catalysts and catalyst supports (*39, 40*). As an example, we show in Figs. 6A and 6B conventional proton-decoupled static and MASS ^{17}O NMR spectra of an X ray amorphous silica sample. The only feature evident in these spectra is the broad second-order quadrupolar powder pattern ($e^2qQ/h \cong 5.8$ MHz, $\eta \cong 0$, $\delta_i \cong 50$ ppm) of the siloxy (Si–O–Si) oxygen sites, similar to the resonance observed for the crystalline SiO_2 polymorph, low cristobalite (*1*). In the amorphous case, however, the siloxy oxygen resonance is asymmetrically broadened, due to a distribution of bond angles and bond lengths (*16*). Using cross polarization with short contact times (0.3 ms or less; Figs. 6C and 6D), we find a previously unobserved resonance for amorphous silica, which we assign to silanol (Si–O–H) sites present both on the surface of the silica and at internal defect sites. This resonance has a smaller quadrupole coupling constant (~4.0 MHz), a larger asymmetry parameter (~0.3), and a more shielded isotropic chemical shift (~20 ppm) than the siloxy oxygen resonance and is masked in the conventional spectra (Figs. 6A and 6B) by the broader, more intense resonance of the latter. To support our assignment of the new resonance to surface silanol groups, we have examined the ^{17}O resonance of the crystalline silanol $(C_6H_5)_3SiOH$, as shown in Figs. 6E and 6F. While this resonance does not display a well-defined second-order quadrupolar lineshape, it does indeed behave like a quadrupolar powder pattern in both its field dependence and its partial narrowing with MASS. We obtain reasonable simulations of these lineshapes using a quadrupole coupling constant of 4.1 MHz, an

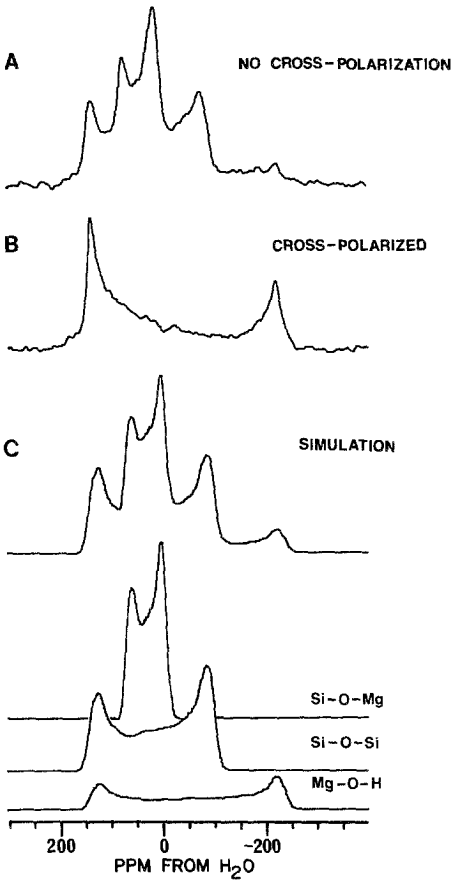

FIG. 5. Static ^{17}O NMR spectra of polycrystalline talc ($Mg_3Si_4O_{10}(OH)_2$) obtained at 67.8 MHz. (A) Proton-decoupled spectrum without cross polarization: 500 scans, 10 s recycle time. (B) Cross-polarized spectrum: 500 scans, 33 μs contact time, 10 s recycle time. (C) Simulated spectrum using three second-order quadrupolar powder patterns with the following parameters: (1) e^2qQ/h = 3.2 MHz, η = 0, δ_i = 40 ppm, relative intensity 2.0; (2) e^2qQ/h = 5.8 MHz, η = 0, δ_i = 50 ppm, relative intensity 3.0; (3) e^2qQ/h = 7.3 MHz, η = 0, δ_i = 0 ppm, relative intensity 1.0.

asymmetry parameter of 0.6, and an isotropic chemical shift of 10 ppm, in agreement with the silanol resonance from silica except for a somewhat larger asymmetry parameter. In further support of our assignment of the resonance of Figs. 6C and 6D to silanol sites, we note that its intensity can be reduced by heating to 200°C and above, where dehydroxylation of silica surfaces is known to occur (*40*). We also observe that, in contrast to the bridging oxygen resonance, the putative silanol resonance is significantly narrowed by proton decoupling, as expected for a hydroxyl oxygen site.

When longer cross-polarization contact times are used, the siloxy oxygen resonance of amorphous silica can also be observed as nonhydroxyl oxygens in the vicinity of the silanol groups begin to cross polarize. These sites have a larger cross-relaxation time constant (see Table 1) as a result of their greater distance from the protons. Our

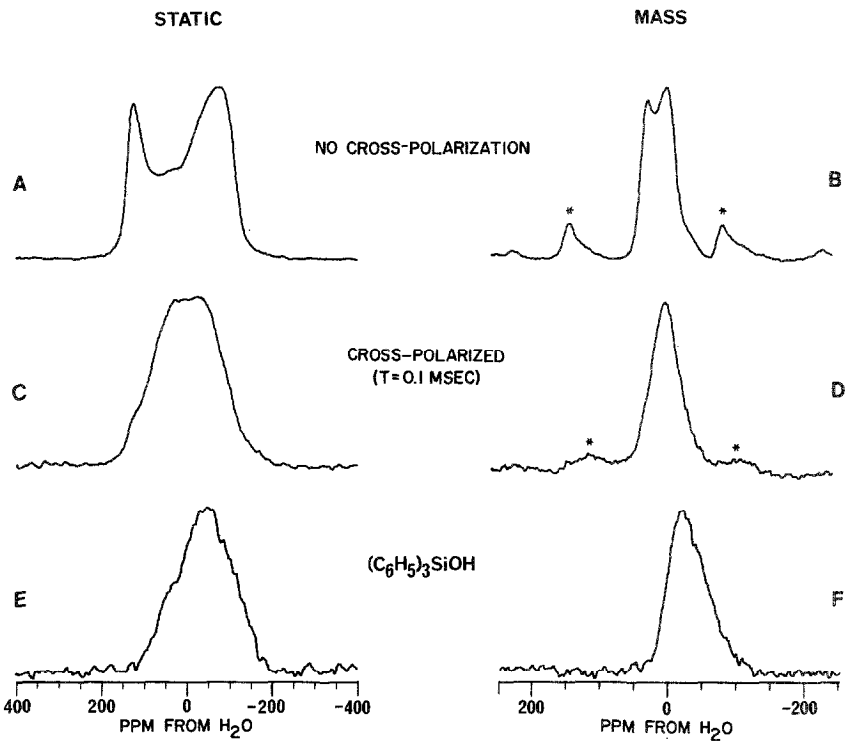

FIG. 6. Static and MASS ^{17}O NMR spectra of amorphous SiO_2 and polycrystalline $(C_6H_5)_3SiOH$ obtained at 67.8 MHz. (A) Proton-decoupled static spectrum of SiO_2 without cross polarization: 108 scans. (B) Proton-decoupled MASS spectrum: 100 scans, 7.6 kHz spinning speed (* indicates spinning sidebands). (C) Cross-polarized static spectrum of SiO_2: 200 scans, 0.1 ms contact. (D) Cross-polarized MASS spectrum: 200 scans, 0.1 ms contact, 7.6 kHz spinning speed. (E) Proton-decoupled static spectrum of $(C_6H_5)_3SiOH$ without cross polarization: 500 scans. (F) Proton-decoupled MASS spectrum of $(C_6H_5)_3SiOH$: 800 scans, 4.0 kHz spinning speed. All spectra were obtained using a 2 s recycle time.

results are consistent with the ^{29}Si cross-polarization results of Maciel and Sindorf (*41*), in which selective observation of surface silicon sites in silica gels was demonstrated. From our own ^{29}Si NMR results on the ^{17}O-enriched silica sample whose spectrum is shown in Fig. 6, we calculate that 14% of the oxygens are in silanol sites, with $\frac{1}{3}$ of these being geminal hydroxyls ($Si(OSi)_2(OH)_2$). The relative intensities of the oxygen resonances shown in Fig. 6 are consistent with these results: noting that the integrated intensity of the cross-polarized silanol resonance in Fig. 6C is smaller than the total intensity of the non-cross-polarized resonance (Fig. 6A) by a factor of 2.7, and assuming a cross-polarization enhancement of 3 (a typical value), we estimate that the silanol resonance accounts for approximately 12% of the total intensity.

CONCLUSIONS

The results presented in this paper represent the first in-depth study of the cross-polarization behavior of noninteger spin quadrupolar nuclei in powders. We have shown that reliable second-order quadrupolar powder patterns can be obtained under

cross-polarization conditions and that significant sensitivity enhancements can be achieved. Cross polarization should be useful for other low γ, low abundance, non-integral spin quadrupolar nuclei such as ^{25}Mg, ^{33}S, and ^{67}Zn, which are difficult to observe by solid-state NMR. We have also shown that the large differences in cross-relaxation rates for oxygen sites with and without directly bonded hydrogen can be exploited to assign hydroxyl oxygen resonances in inorganic samples. This approach is very useful in interpreting the ^{17}O NMR spectra of a variety of phyllosilicates, such as talc, chrysotile, and phlogopite, as well as the aluminum cluster $Na\text{-}[Al_{13}O_4(OH)_{24}(H_2O)_{12}](SeO_4)_4 \cdot 13H_2O$ (*42*). We expect that ^{17}O cross-polarization NMR should also be useful for studies of organic compounds. Although organic species generally have ^{17}O nuclear quadrupole coupling constants that are considerably larger than those of the inorganic compounds described above (*2*), we have been able to observe ^{17}O resonances for ^{17}O-enriched myristic acid ($CH_3(CH_2)_{12}COOH$) and myristic anhydride using dipolar decoupling and cross polarization. We have also demonstrated here that ^{17}O cross polarization enables the observation of previously undetectable surface hydroxyl oxygen resonances in high surface area metal oxides. The ability to directly probe surface oxygen sites may provide new insight into the dehydration/rehydration behavior of amorphous silica, since one can readily distinguish between hydroxyl groups and adsorbed water. With the surface selectivity afforded by cross polarization, it may also be possible to use ^{17}O NMR to observe changes in the surface structure of metal oxides upon adsorption of organic species or metal crystallites, affording an insight into surface interactions important in heterogeneous catalysis.

APPENDIX

In order to discuss the details of the cross-polarization dynamics for ^{17}O we follow the general derivation given by Mehring (*33*). Starting with the assumption that the oxygen inverse spin temperature, β_O, simultaneously relaxes toward the instantaneous proton inverse spin temperature, β_H, with a time constant T_{OH} and decays with a time constant $T_{1\rho}^O$, the following differential equations can be written:

$$(d/dt)\beta_O = -1/T_{OH}(\beta_O - \beta_H) - (1/T_{1\rho}^O)\beta_O$$

$$(d/dt)\beta_H = -\epsilon\alpha^2/T_{OH}(\beta_H - \beta_O) - (1/T_{1\rho}^H)\beta_H. \qquad [A1]$$

With the initial conditions $\beta_O(t = 0) = 0$ and $\beta_H(t = 0) = \beta_{H,i}$, the solution is

$$\beta_O(t) = \beta_{H,i}(a_+ - a_-)^{-1}[\exp(-a_-t/T_{OH}) - \exp(-a_+t/T_{OH})], \qquad [A2]$$

where

$$a_\pm = c[1 \pm (1 - b/c^2)^{1/2}]$$

$$b = (T_{OH}/T_{1\rho}^H)(1 + T_{OH}/T_{1\rho}^O) + \epsilon\alpha^2(T_{OH}/T_{1\rho}^O)$$

$$c = \tfrac{1}{2}(1 + \epsilon\alpha^2 + T_{OH}/T_{1\rho}^H + T_{OH}/T_{1\rho}^O)$$

$$\epsilon = N_O/3N_H$$

$$\alpha = 3\gamma_O H_{1O}/\gamma_H H_{1H}. \qquad [A3]$$

The quantity α is the Hartmann–Hahn mismatch parameter, which is 1 when Eq. [1] is satisfied, ϵ is the ratio of the ^{17}O and ^1H spin heat capacities, and N_O and N_H are

the number of ^{17}O and ^{1}H nuclei, respectively. The definitions of α and ϵ have been modified from those of Mehring to account for the fact that only the central $(\frac{1}{2}, -\frac{1}{2})$ transition of the ^{17}O nucleus is being cross polarized in our experiments, and the symbol c has been substituted for Mehring's a_0.

The oxygen magnetization M_O is related to β_O by

$$M_O(t) = \alpha(\gamma_H/\gamma_O)(\beta_O(t)/\beta_{H,i})M_{O,e}, \quad [A4]$$

where $M_{O,e}$ is the equilibrium oxygen spin magnetization obtained by a single 90° pulse. Substituting from Eqs. [A2] and [A3] gives

$$M_O(t) = \alpha(\gamma_H/\gamma_O)M_{O,e}(a_+ - a_-)^{-1}[\exp(-a_-t/T_{OH}) - \exp(-a_+t/T_{OH})]. \quad [A5]$$

When $T_{OH}/T_{1\rho}^O$ and $\epsilon\alpha^2$ are both negligible, this equation reduces to

$$M_O(t) = \alpha(\gamma_H/\gamma_O)M_{O,e}(1 - T_{OH}/T_{1\rho}^H)^{-1}[\exp(-t/T_{1\rho}^H) - \exp(-t/T_{OH})]. \quad [A6]$$

This is the conventional form that we have used for fitting the contact time data. We show above, however, that the $T_{OH}/T_{1\rho}^O$ term cannot always be neglected in ^{17}O cross polarization. It is also clear that in these highly ^{17}O-enriched inorganic samples the $\epsilon\alpha^2$ term becomes significant. When both of these terms are nonnegligible, Eq. [A5] cannot be further simplified. However, when the $\epsilon\alpha^2$ term alone is negligible, the general equation reduces to

$$M_O(t) = \alpha(\gamma_H/\gamma_O)M_{O,e}(1 + T_{OH}/T_{1\rho}^O - T_{OH}/T_{1\rho}^H)^{-1}[\exp(-t/T_{1\rho}^H) - \exp(-t(1/T_{OH} + 1/T_{1\rho}^O))]. \quad [A7]$$

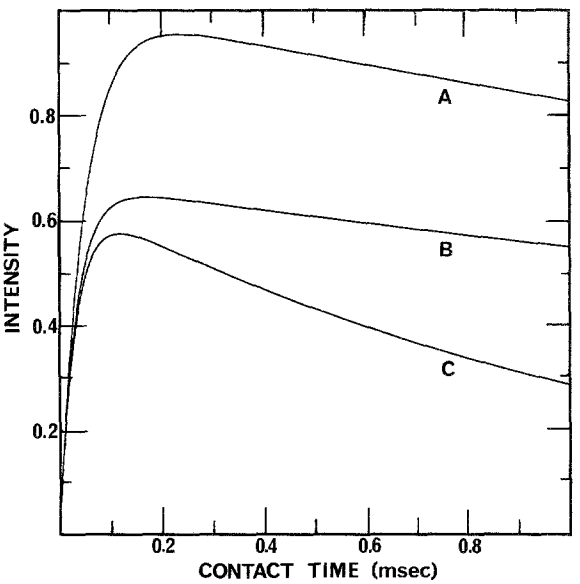

FIG. 7. Simulated contact time curves: (A) Curve based on Eq. [A6] with T_{OH} = 0.050 ms, $T_{1\rho}^H$ = 5.0 ms. (B) Curve based on Eq. [A7] with $T_{1\rho}^O$ = 0.10 ms and same T_{OH} and $T_{1\rho}^H$ values. (C) Curve based on Eq. [A5] with $\epsilon\alpha^2$ = 0.10 and same T_{OH}, $T_{1\rho}^H$, and $T_{1\rho}^O$ values. The ordinate in each case is $M_O(t)/[\alpha(\gamma_H/\gamma_O)M_{O,e}]$.

This equation differs from Eq. [A6] in two respects: first, the time constant for cross relaxation is $(1/T_{OH} + 1/T^{O}_{1\rho})^{-1}$ rather than T_{OH}, and second, the preexponential constant contains the additional term $T_{OH}/T^{O}_{1\rho}$. The consequences of these differences are that the ^{17}O magnetization builds up at a faster rate, but the maximum value attained is reduced by the factor $(1 + T_{OH}/T^{O}_{1\rho} - T_{OH}/T^{H}_{1\rho})/(1 - T_{OH}/T^{H}_{1\rho})$. These points are illustrated in the simulated contact time curves of Fig. 7.

Inclusion of the $\epsilon\alpha^2$ term in Eq. [A5] has the effect of further decreasing both the cross-relaxation time constant and the maximum intensity, as illustrated in Fig. 7. It can also be seen, however, that inclusion of this term also results in a shorter apparent $T^{H}_{1\rho}$. It is evident from Fig. 7 (and Eq. [A5]) that in all three cases the contact time dependence has the same functional form, i.e., the difference of two exponentials. Thus there is nothing in the experimentally determined contact time curves to indicate that contributions from either $T^{O}_{1\rho}$ or $\epsilon\alpha^2$ are significant, and they must consequently be evaluated by independent measurements, as we have done for $T^{O}_{1\rho}$. While it is possible to calculate the true T_{OH} and $T^{H}_{1\rho}$ values from the experimentally determined time constants T'_{OH} and $T^{H'}_{1\rho}$, together with independently measured $T^{O}_{1\rho}$ and $\epsilon\alpha^2$ values, we have chosen to report only the effective values T'_{OH} and $T'_{1\rho}$, since it is these parameters that govern the actual cross-polarization dynamics.

ACKNOWLEDGMENTS

We thank Mr. C. Weiss, Jr., and Professor R. J. Kirkpatrick for the generous loan of their ^{17}O-talc sample, Mr. B. Phillips for valuable advice on crystal structures and for obtaining powder X ray diffraction spectra, Dr. S. Schramm and Dr. Kirk Schmitt for use of their ^{17}O-$(C_6H_5)_3SiOH$ sample, and Dr. C. T. G. Knight for the loan of his ^{17}O-SiO_2, as well as for helpful discussions.

REFERENCES

1. S. SCHRAMM, R. J. KIRKPATRICK, AND E. OLDFIELD, *J. Am. Chem. Soc.* **105,** 2483 (1983).
2. S. SCHRAMM AND E. OLDFIELD, *J. Am. Chem. Soc.* **106,** 2502 (1984).
3. G. E. MACIEL, B. L. HAWKINS, J. S. FRYE, AND C. E. BRONNIMANN, "Abstracts of Papers, 25th Experimental NMR Conference, Wilmington, Delaware, 1984"; Abstract II-B-14.
4. G. L. TURNER, S. E. CHUNG, AND E. OLDFIELD, *J. Magn. Reson.* **64,** 316 (1985).
5. H. K. C. TIMKEN, G. L. TURNER, J.-P. GILSON, L. B. WELSH, AND E. OLDFIELD, *J. Am. Chem. Soc.* **108,** 7231 (1986).
6. H. K. C. TIMKEN, N. JANES, G. L. TURNER, S. L. LAMBERT, L. B. WELSH, AND E. OLDFIELD, *J. Am. Chem. Soc.* **108,** 7236 (1986).
7. J. KLINOWSKI, J. M. THOMAS, S. RAMDAS, C. A. FYFE, AND G. C. GOBBI, *in* "Second Workshop on the Adsorption of Hydrocarbons in Microporous Sorbents," Eberswalde, G.D.R., 1982; Vol. 2, Supplement.
8. J. KLINOWSKI, *Prog. NMR Spectrosc.* **16,** 237 (1984).
9. H. K. C. TIMKEN, S. E. SCHRAMM, R. J. KIRKPATRICK, AND E. OLDFIELD, *J. Phys. Chem.* **91,** 1054 (1987).
10. N. JANES AND E. OLDFIELD, *J. Am. Chem. Soc.* **108,** 5743 (1986).
11. A. PINES, M. G. GIBBY, AND J. S. WAUGH, *J. Chem. Phys.* **59,** 569 (1973).
12. E. O. STEJSKAL AND J. SCHAEFER, *J. Magn. Reson.* **18,** 560 (1975).
13. E. O. STEJSKAL, J. SCHAEFER, AND T. R. STEGER, *Faraday Soc. Symp.* **13,** 56 (1979).
14. E. FUKUSHIMA AND S. B. W. ROEDER, "Experimental Pulse NMR," p. 174, Addison–Wesley, Reading, Massachusetts, 1981.
15. A. AVOGADRO AND A. RIGAMONTI, *in* "Magnetic Resonance and Related Phenomena" (V. Hovi, Ed.), p. 255, North-Holland, Amsterdam, 1973.
16. A. E. GEISSBERGER AND P. J. BRAY, *J. Non-Cryst. Solids.* **54,** 121 (1983).

17. J. SCHAEFER, R. A. MCKAY, AND E. O. STEJSKAL, *J. Magn. Reson.* **34,** 443 (1979).
18. M. G. GIBBY, A. PINES, AND J. S. WAUGH, *J. Am. Chem. Soc.* **94,** 6231 (1972).
19. W. P. ROTHWELL, J. S. WAUGH, AND J. P. YESINOWSKI, *J. Am. Chem. Soc.* **102,** 2637 (1980).
20. T. T. P. CHEUNG, L. E. WORTHINGTON, P. D. MURPHY, AND B. C. GERSTEIN, *J. Magn. Reson.* **41,** 158 (1980).
21. T. K. PRATUM AND M. P. KLEIN, *J. Magn. Reson.* **55,** 421 (1983).
22. S. VEGA, T. W. SHATTUCK, AND A. PINES, *Phys. Rev. A* **22,** 638 (1980).
23. P. BRUNNER, M. REINHOLD, AND R. R. ERNST, *J. Chem. Phys.* **73,** 1086 (1980).
24. S. VEGA, *Phys. Rev. A* **23,** 3152 (1981).
25. C. S. BLACKWELL AND R. L. PATTON, *J. Phys. Chem.* **88,** 6135 (1984).
26. R. G. BRYANT, S. GANAPATHY, AND S. D. KENNEDY, *J. Magn. Reson.* **72,** 376 (1987).
27. D. W. WOESSNER, *Z. Phys. Chem. N.F.,* in press.
28. S. R. HARTMANN AND E. L. HAHN, *Phys. Rev.* **128,** 2042 (1962).
29. V. H. SCHMIDT, *in* "Proceedings of the Ampère International Summer School II: Pulsed Magnetic and Optical Resonance" (R. Blinc, Ed.), p. 75, University of Ljubljana, Ljubljana, Yugoslavia, 1972.
30. G. H. STRAUSS, *J. Chem. Phys.* **40,** 1988 (1964).
31. J. D. BERNAL AND H. D. MEGAW, *Proc. R. Soc. London A* **151,** 384 (1935).
32. W. R. BUSING AND H. A. LEVY, *J. Chem. Phys.* **26,** 563 (1957).
33. M. MEHRING, "Principles of High Resolution NMR in Solids," 2nd ed., p. 151, Springer-Verlag, Berlin, 1983.
34. L. B. ALEMANY, D. M. GRANT, R. J. PUGMIRE, T. D. ALGER, AND K. W. ZILM, *J. Am. Chem. Soc.* **105,** 2133 (1983).
35. L. MÜLLER, A. KUMAR, T. BAUMANN, AND R. R. ERNST, *Phys. Rev. Lett.* **32,** 1402 (1974).
36. D. C. AILION, *in* "Advances in Magnetic Resonance" (J. S. Waugh, Ed.), Vol. 5, p. 177, Academic Press, New York, 1971.
37. G. G. CHRISTOPH, C. E. CORBATO, D. A. HOFMANN, AND R. T. TETTENHORST, *Clays Clay Miner.* **27,** 81 (1979).
38. J. H. RAYNER AND G. BROWN, *Clays Clay Miner.* **21,** 103 (1973).
39. B. C. GATES, J. R. KATZER, AND G. C. A. SCHUIT, "Chemistry of Catalytic Processes," McGraw–Hill, New York, 1979.
40. C. OKKERSE, *in* "Physical and Chemical Aspects of Adsorbents and Catalysts" (B. G. Linsen, Ed.), p. 213, Academic Press, London, 1970.
41. G. E. MACIEL AND D. W. SINDORF, *J. Am. Chem. Soc.* **102,** 7606 (1980).
42. A. R. THOMPSON, A. C. KUNWAR, H. S. GUTOWSKY, AND E. OLDFIELD, *J. Chem. Soc., Dalton Trans,* in press.